Materials Research Express

PAPER

Large-scale self-assembled epitaxial growth of highly-ordered three-dimensional micro/nano single-crystalline PbSe pyramid arrays by selective chemical bath deposition

RECEIVED
3 February 2015

REVISED
15 April 2015

ACCEPTED FOR PUBLICATION
22 April 2015

PUBLISHED
19 May 2015

Jijun Qiu[1,5], **Binbin Weng**[1,5], **Lin Li**[2], **Xiaomin Li**[3] **and Zhisheng Shi**[1,4]

[1] School of Electrical and Computer Engineering, University of Oklahoma, Norman, Oklahoma 73019, USA
[2] Key Laboratory for Photonic and Electronic Bandgap Materials, Ministry of Education, School of Physics and Electronic Engineering, Harbin Normal University, Harbin 150025, People's Republic of China
[3] State Key Laboratory of High Performance Ceramics and Superfine Microstructures, Shanghai Institute of Ceramics, Chinese Academy of Sciences, Shanghai, 200050, People's Republic of China
[4] Nanolight Inc., Norman, Oklahoma 73069, USA
[5] J. Qiu and B. Weng contributed equally to this work

E-mail: jjqiu@ou.edu **and** shi@ou.edu

Keywords: pyramid arrays, lead salt, epitaxial growth, chemical bath deposition, oriented attachment

Abstract

Highly ordered three-dimensional micro- and nano- PbSe pyramid arrays were synthesized by using selective epitaxial self-assembled chemical bath deposition method. Each pyramid consists of a very sharp (111) tip with six smooth equivalent {100} facets. Every (100) facet forms an angle of about 54.7° with respect to the (111) facet. The structural features including pyramidal size and period could be precisely tailored by pre-patterned Au mask and etching time. Pyramids are self-assembled on the confined positions by the dual functions of one-dimensional and two-dimensional oriented attachment mechanisms along [110] directions on the (111) surface, following the Gibbs-Curie-Wulff minimum energy principle. This method could effectively create large, bottom-up 3D pyramidal surface patterns in a cost-effective and time-saving manner, which has potential applications in infrared photoconductors, solar cells and light emitting enhancement for display, etc.

1. Introduction

Precise control of three-dimensional (3D) pyramid surface patterns is increasingly important in optoelectronic devices [1] such as solar cells [2, 3], detectors [4], light-emitting diodes [5, 6], and triboelectric nanogenerators [7]. For example, as an anti-reflection coating, the pyramidal or inversed pyramidal surface pattern not only significantly improves the silicon solar cells performances by improving the light trapping, but also reduces the thickness of silicon by more than 90 percent for solar cells applications while still maintaining the high efficiency [8]. In contrast to two-dimensional disk and rings, hexagonal gallium nitride (GaN) pyramids are 3D cavities which could be designed to emit a beam from each of smooth sides, and generate higher quantum efficiency [9]. Despite of the unique attractive properties of 3D pyramidal structures, materials that have been successfully surface-textured with ordered 3D pyramidal units are very limited. This is mainly due to challenges in creating 3D pyramidal structures through traditional lithography-etching techniques, including plasma etching [10], chemical etching [11], reactive ion etching [12], and laser engraving [13, 14].

In this work, for the first time, we successfully demonstrate that large-area ordered 3D pyramidal surface patterns can be readily realized by wet-chemical selective epitaxial self-assembled growth. Lead selenide (PbSe) is a promising material for many applications [15], including laser materials [16], thermo-electric devices [17], and infrared (IR) detectors [18], Recently, the discovered phenomenon of the multiple exciton generation (MEG) effect in PbSe nanocrystals could lead to an entirely new paradigm for ultra high efficiency of 65% (about 800% quantum efficiency limit) and low-cost solar cell technology [19, 20]. This discovery further stirs up the enthusiasm for developing new technologies to precisely control the size, density, shape and dimension of PbSe

surface pattern, expecting for not only a further improvement of the performance of the established PbSe devices, but also the exploration of a new physical mechanism for the design and fabrication of next generation devices.

Up to date, one-dimensional (1D) pillar PbSe surface patterns have been successfully obtained by etching single-crystalline PbSe films synthesized from molecular beam epitaxy (MBE) method [21], however, there is still no report about fabrication of 3D PbSe surface patterned structure. On the other hand, the chemical bath deposition (CBD) [22–25] is a well-known method generally used to fabricate poly-crystalline PbSe films and free-substrate particles with different shapes [26–28], such as cubes, truncated octahedrons, octahedron and dendrite-like structures. Compared with top-down etching method, bottom-up CBD epitaxial self-assembly is a more desirable technology for next generation nano-structuring applications, due to easy synthesis together with a large versatility in the physic-chemistry of the respective materials. Therefore, in this work, CBD method is adopted to textured pyramid PbSe surface pattern via surface epitaxial self-assemble engineering. The experiment results show that the method can be used to create large-area and very uniform pyramid patterns with multiple structure-controlling capabilities. The size, density, morphology and surface roughens of pyramids can be conveniently adjusted by varying the selective growth area, growth time and etching time.

2. Experimental details

Our fabrication process mainly involves a selectively epitaxial self-assembled chemical growth on the patterned PbSe epitaxial layer and an isotropy wet-chemical etching. A schematic illustration of the fabrication process is depicted in figure 1. First of all, a high quality mono-crystalline (111) PbSe epitaxial layer was deposited on Shiraki-cleaned (111) silicon wafer by using molecular beam epitaxy (MBE) method (figure 1(a-1)). Secondly, Au mask with patterned circular or quadrate holes was coated over the (111) PbSe epitaxial layer by using UV-lithography (figure 1(a-2)), metal evaporation and lift off processes (figure 1(a-3)) in orders. Finally, highly ordered 3D PbSe pyramid arrays with uniform size were sculptured after chemical bath deposition (figure 1(a-4)) followed with an wet etching process (figure 1(a-5)).

2.1. Fabrication of 3D PbSe pyramid arrays

2.1.1. Deposition of epitaxial PbSe layer on Si (111) substrate

Mono-crystal (111) PbSe epitaxial layer was grown on the (111) Si substrate by a custom-designed MBE apparatus with a compound source of PbSe and an element source of Se [29]. Prior to the deposition, a single-sided polished Si (111) substrate was cleaned by using modified Shiraki cleaning method. After an appearance of 7×7 reconstruction reflection high-energy electron diffraction (RHEED) pattern, a 2 nm thick CaF2 layer was then grown at 750 °C with a 2.5Å/sec growth rate. Subsequently, a 10% Se-to-PbSe flux ratio was used for the growth of the PbSe thin films at substructure temperature of 380 °C with a growth rate of 1.2 μm h^{-1}.

2.1.2. Fabrication of Au mask with patterned holes over the MBE- (111) PbSe epitaxial layer

A positive photoresist (AZ 400 K) layer was coated onto epitaxial PbSe layer by spin-coating at 5000 rpm for 60 s followed by a soft bake for 5 min at 90 °C, as shown in figure 1(a-2). Then circular or quadrate photoresist arrays with various sizes and periods were patterned by using UV lithography (275 W) with an exposure time of 11 s, followed by a development time of 45 s. Subsequently, 30 nm thick Au layer was deposited on the photoresist pattern by employing evaporation at room temperature for 10 mins in 2×10^{-4} Pa. Finally, a patterned Au masks with circular or quadrate hole arrays, where exposed the underlying epitaxial PbSe layer, were obtained after life off in acetone solvent for 5 mins, as shown in figure 1(a-3).

2.1.3. Selective epitaxial growth of PbSe pyramid array

Ordered 3D PbSe pyramid arrays were synthesized by directly immersing the patterned substrates into the CBD growth solution. The aqueous precursor was prepared via dissolving sodium hydroxide, lead acetate and selenosulfate with a concentration ratio of 12:1:1. The resultant patterned substrates were immersed upside down into the aqueous precursor and maintained at 70 °C for 3 h. After reaction was over, large-size PbSe pyramids were grown from the circular or quadrate holes, coupling with small-size free-oriented PbSe particles with various shapes on the Au masks, as shown in figures 1(a-4) and 1(c). Ordered and neat 3D PbSe pyramid arrays were obtained after getting rid of small-size PbSe particles by a wet-chemical etching solution at room temperature for various times, as shown in figures 1(a-5) and 1(d).

2.2. Characterization of 3D PbSe pyramid arrays

The morphological features of 3D PbSe pyramids were observed by using field emission scanning electron microscope (FESEM, Zeiss Neon-40 EsB) with electron backscattered diffraction (EBSD). The crystalline

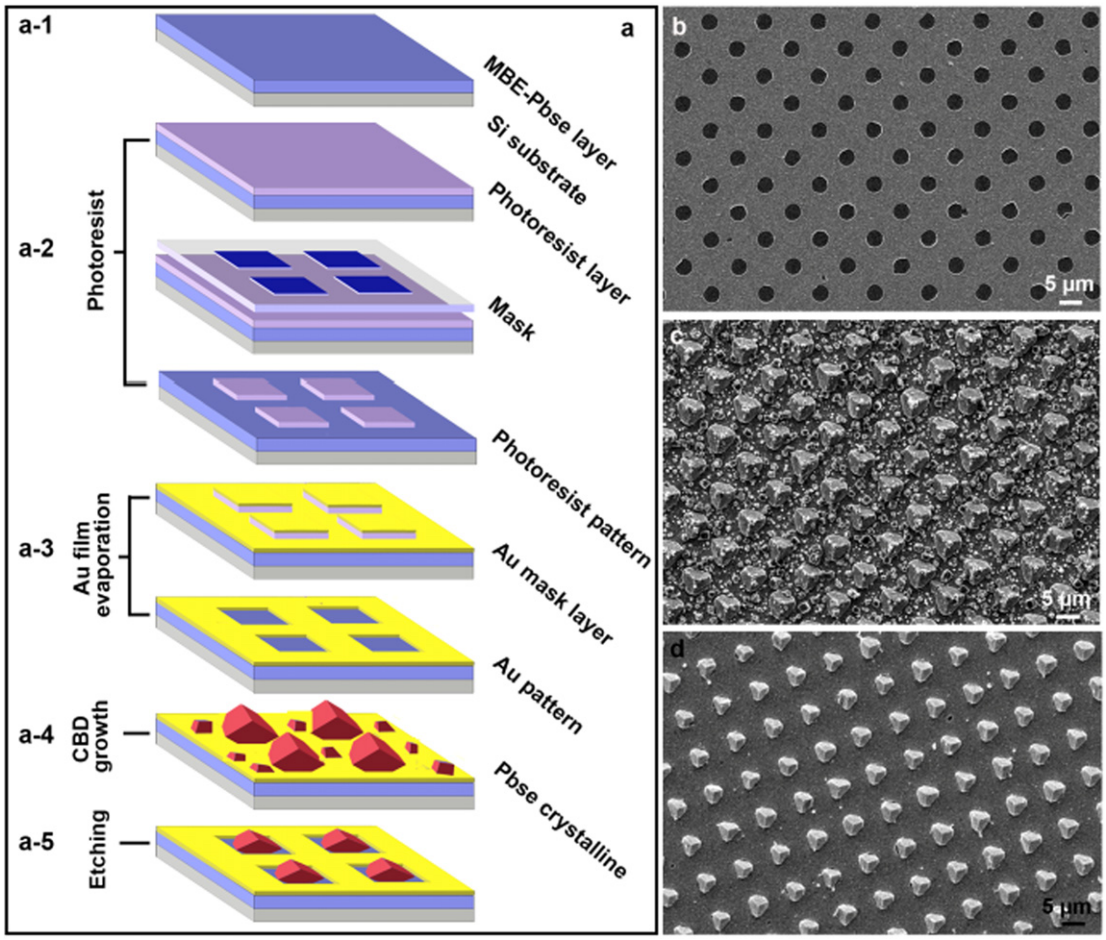

Figure 1. Schematic illustration and FESEM images of highly ordered 3D PbSe pyramidal arrays. (a) Schematic illustration of the fabrication process by using selective epitaxial self-assembled chemical bath deposition. (b) Top-view FESEM image of Au mask with patterned circular holds over MBE-(111) PbSe epitaxial layer. (c) Top-view FESEM image of unretouched 3D PbSe pyramidal arrays after CBD growth, coupling with small non-oriented PbSe particles. (d) Top-view FESEM image of highly neat 3D PbSe pyramidal arrays after chemical etching.

structure was examined by a high resolution Bruker D8 Discover (Cu Kα radiation, $\lambda = 1.5406$ Å) x-ray diffractometer (XRD).

3. Results and Discussion

3.1. Structural and optical characterizations of 3D PbSe pyramid arrays.

Figure 2 shows a typical 3D PbSe pyramid arrays self-assembled from Au mask with 8×8 μm square holes arrays and 50 μm periods. It is clearly that all PbSe islands exhibit a highly uniform size distribution and well-defined pyramidal shape. High magnification tiled FESEM images from various viewing angles in figures 2(c)–(e) reveal the fact that the pyramid is assembled with three large inward and three small outward faces. The three larger faces with a pentagonal section are perpendicular to each other and converge into a sharp tip, being the peak of the pyramid. Three smaller faces are of a regular triangular shape, and each of smaller faces is perpendicular with the two adjacent large faces and is parallel with the remaining large face. All side facets are inclined by 54.7° with respect to the substrate (111) MBE-PbSe epitaxial layer.

The growth orientation of the PbSe pyramid was investigated by the EBSD, as shown in figures 1(f) to (h). A clearly resolved Kikuchi line was observed in figure 1(f), and matched well with the Kikuchi pattern of (100) oriented EBSD-calculated PbSe unit cells shown in figure 1(g), suggesting the face is mono-crystalline (100) face. Moreover, EBSD inverse pole figure (IPF) mapping of (100) plane in figure 1(h) reveals a pure color, indicating a high uniformity of (100)-orientation.

Additionally, only (111) peaks, including higher orders up to (333), were observed in the XRD patterns of 3D PbSe pyramid arrays, as shown in figure 1(i), indicating that these pyramids are in good alignment and mono-crystalline.

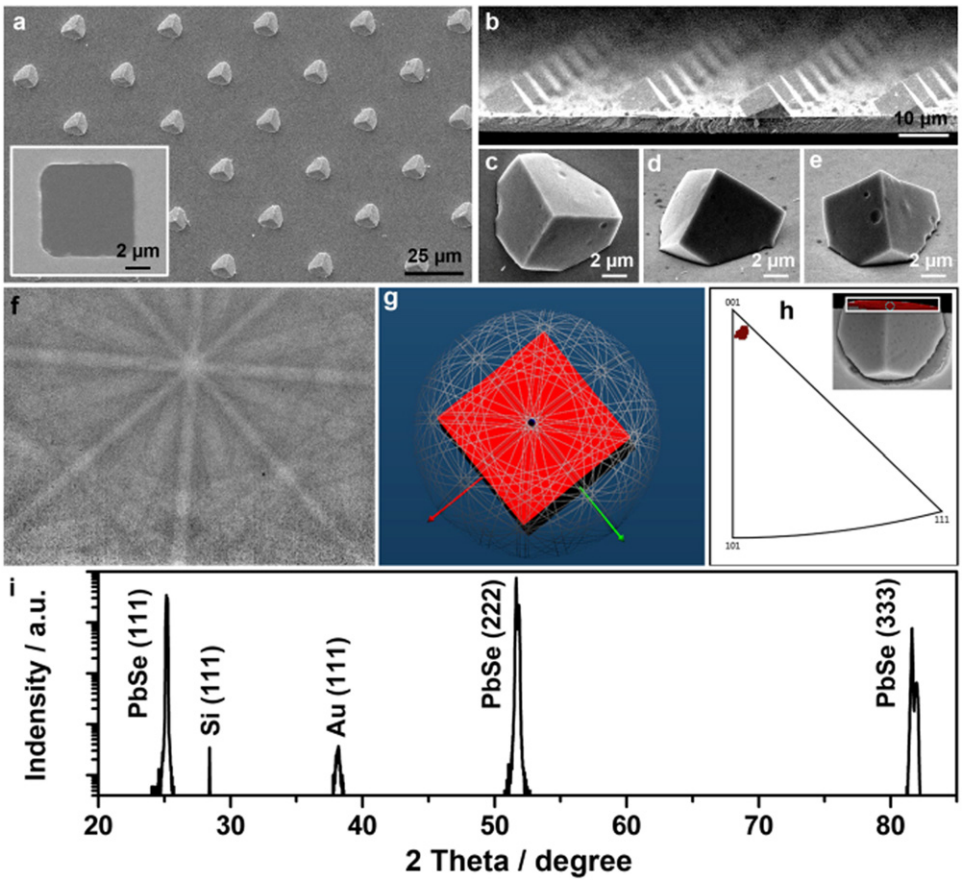

Figure 2. Morphological and crystal characteristics of 3D PbSe pyramidal arrays. Low-magnification (a) top-veiw and (b) side-view FESEM images of PbSe pyramid arrays. (c), (d) and (e) High-magnification titled-view FESEM image of individual PbSe pyramid from various viewing angles. (f) Experimental EBSD Kikuchi pattern captured from an individual PbSe pyramid. (g) Kikuchi pattern of (100) oriented EBSD-calculated unit cells. (h) Inverse pole figure (IPF) mapping from one of large PbSe planes shown in top right corner. (i) XRD pattern of ordered 3D pyramid arrays on patterned MBE-(111) PbSe epitaxial layer buffered (111) Si substrate.

Above crystal structure characteristics demonstrate that the pyramid are formed by six {100} surface planes, and these facets are all aligned parallel to the sixfold [110] directions within the (111) surface plane. This is consistent with the fact that the {100} planes are the lowest free energy surfaces for the lead salt compounds.

Figure 3 demonstrates an interesting phenomenon of the light reflection behaviors from the Si substrate with 3D PbSe pyramid arrays. The substrate was fixed on a rotatable stage, and each of the images was taken while the wafer turned in every 30°. As can be seen, the change of reflection intensity cycles three times (0°, 120° and 240°) when the substrate rotates in 360°. This phenomenon is due to the well aligned pyramid array structure as shown in previous FESEM images. For one individual pyramid structure, the three big {100} oriented planes are perpendicular to each other. And every micro-structure has the same orientation and well-aligned to form a hexagonal array. Therefore, when one of the big {100} plane faces right at the camera, the visible light is guided to the camera lens and reflection strength becomes strongest, as shown in pictures at 0, 120, and 240° respectively. And when the edges connecting the {100} planes face at the camera, light is reflected away from the camera lens, in this case, the brightness decrease to the weakest, as shown in pictures at 60, 180, and 300°.

3.2. Effect of mask shape and size on the morphology of 3D PbSe pyramid array

Ordered circle- or square-shape hole array patterns with various sizes and periods were obtained after lithography, Au evaporation and lift-off in turn, as shown in figure 1. The size and the period, which are determined by designed sizes of lithography mask, are various in the range from 5 to 20 μm and from 5 to 50 μm, respectively. Figure 4 show the typical FESEM image of 3D PbSe pyramid arrays patterned from round hole arrays with 5 and 2 μm diameters, respectively. Obviously, the mask shape and size have little effect on the morphology of PbSe pyramid, while a nearly linear relation is revealed between mask and pyramid sizes.

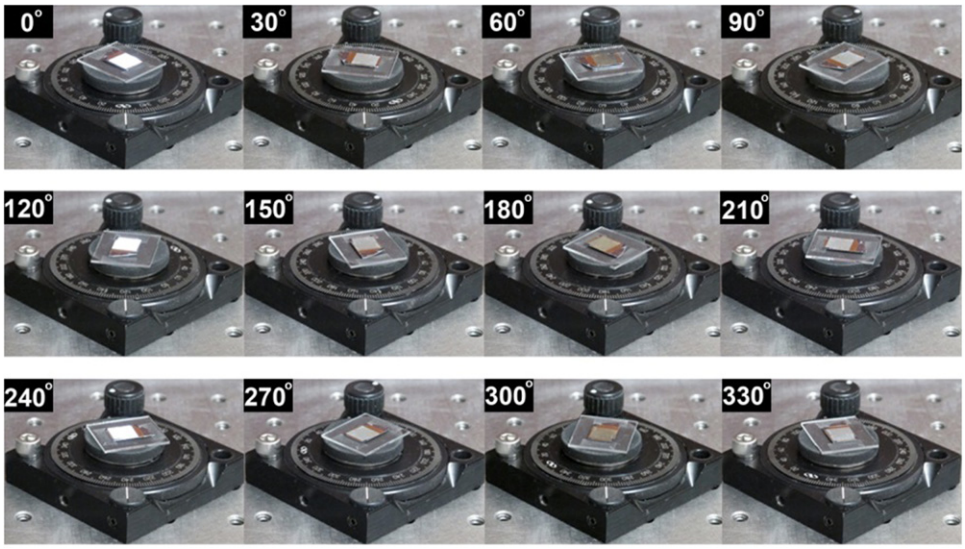

Figure 3. Light reflection behaviors of 3D PbSe pyramid arrays observed from various viewing angle.

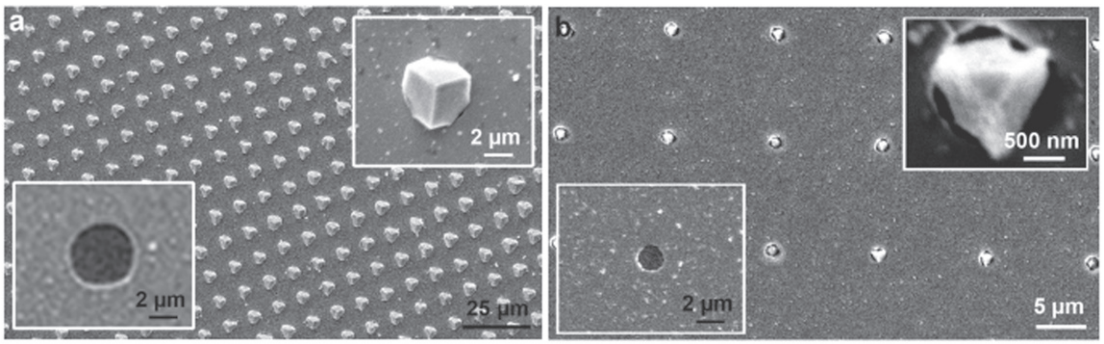

Figure 4. Top-view FESEM images of 3D PbSe pyramid array with various sizes. (a) Large and (b) small PbSe pyramid arrays grown from patterned Au mask with 5 and 2 μm diameter, respectively. The high magnification FESEM images of Au patterns with various hold sizes and the corresponding PbSe pyramids were shown in the bottom-left and top right-corners, respectively.

3.3. Effect of MBE seed layer on the morphology of 3D PbSe pyramid arrays

The patterned MBE-PbSe buffer is essential for the formation of 3D PbSe pyramid arrays. Without MBE-PbSe exipital buffer layer, CBD-grown PbSe films would be polycrystalline material. Figure 5(a) shows PbSe film synthesized on the Si substrate with a coarse surface mophorlogy. The film is 1.2 μm thicknesses, and is composed of PbSe cubic particles with similar sizes varying from 0.5 to 3 μm under different growth conditions. Three peaks with similar intensity were observed from XRD pattern of PbSe films in figure 5(f), which are attributed to PbSe (111), (200) and (220) plane diffractions respectively, indicating that the film is poly-crystalline without oriented growth. With MBE PbSe (111) epitaxial buffer layer substrate, a mono-crystalline PbSe film was obtained as shown in figure 5(d). No boundary is observed between MBE-PbSe and CBD-PbSe layers. After deposition of CBD-PbSe, XRD measurement shows monocrystalline film with only corresponding {111} peaks observed, as shown in figure 5(f). Moreover, a high resolution XRD rocking curve in figure 5(g) shows a narrower line width of 0.06° compared to that of MBE layer, indicating a higher crystalline quality. These results show that a higher quality mono-crystalline (111) PbSe epitaxial layer could be obtained from CBD method by growing on (111) MBE-PbSe epitaxial buffer layer. The single-crystal lead salt films obtained from CBD method were reported by Golan [30–35].

Interestingly, 14 nm min^{-1} growth rate of CBD-PbSe epitaxial layer on MBE substrate is 3 times faster than the typical growth rate of poly-crystalline film on substrate without epitaxial buffer layer. Therefore, compared with MBE technique, CBD growth on MBE epitaxial buffer layer is a promising technique for fabrication of low-cost, high quality and thicker PbSe epitaxial layer, in addition to providing a new way to bottom-up growth of highly ordered mono-crystalline PbSe pyramid arrays.

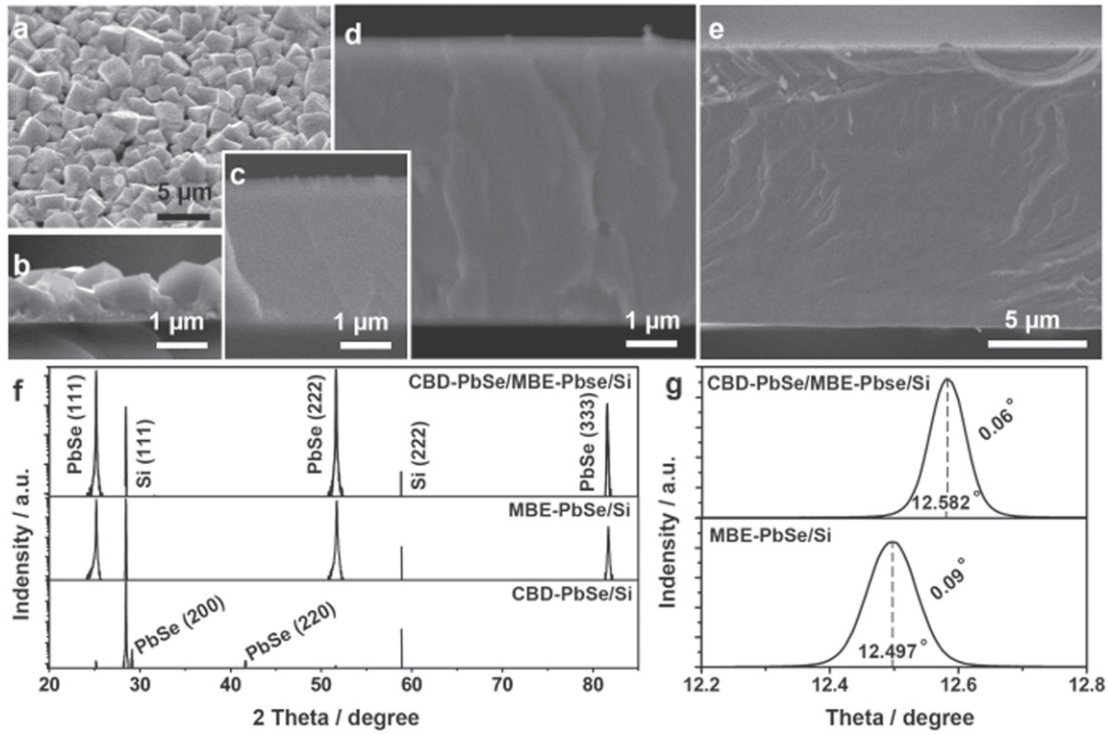

Figure 5. Effect of seed layer on the crystal structure and growth orientation of PbSe material from chemical solution method. (a) Top- and (b) side-view FESEM images of poly-crystalline PbSe films grown from seed-free (111) Si substrates. Side-view FESEM images of (c) MBE-(111) PbSe epitaxial layer and CBD-(111) PbSe epitaxial films with (d) 6 μm and (e) 30 μm thickness. (f) XRD patterns and (g) (111) peak rocking curves of PbSe films fabricated from MBE and CBD methods, respectively.

3.4. Effect of etching to size and shape of 3D PbSe pyramids

It was found that wet-etching is also an effective way to tailor the pyramid size, as shown in figure 6. After 3 h CBD growth, for example, medium 3D PbSe pyramids with maximum 10 μm edge length epitaxially grew from 5×5 μm square hole mask, as shown in figure 6(f). After initial 5 min etching at room temperature, the size decreased to 6 μm with a 0.8 μm min^{-1} etching speed (figure 6(g)). Then the etching speed reduces to 0.35 μm min^{-1} in a subsequent 15 min etching, resulting in 300 nm nano pyramids (figure 6(j)). Furthermore, the PbSe pyramidal morphologies do not any change before and after etching, indicating an isotropic etching.

3.5. Growth process and mechanism of 3D PbSe pyramid array by CBD assisted selective (111) MBE-PbSe epitaxial layer

Here, a 8×8 μm square hole array pattern was utilized to illustrate the process growth of 3D PbSe pyramid arrays. After growth for 15 min, CBD-PbSe not only fill up the squared hole, but also form a high-platform with asymmetric hexagon shape, as shown in figure 7(b). Based on structural characterization mentioned above, we can confirm that the high-platform above Au mask surface is made of a big inward tilt (100) facet, two small inward tilt (100) facets, an outward tilt (100) facet and two uncertain vertical facets, as shown in figure 7(b). Two small inward tilt (100) at the two of corners of square Au mask terminate the intersection of two parallel uncertain vertical facets and the outward tilt (100), which is parallel to the big inward tilt (100) facet. After growth for 30 mins, the two small inward-tilt (100) facets expand quickly both in horizontal and vertical directions, and reach the same size with the bigger one which just has an obvious expansion in the vertical direction. The two parallel unknown vertical facets disappear, meanwhile, the other two outward-tilt (100) facets with irregular shape emerge at the both ends of original big (100) facet during the expansion of two small (100) facets, as shown in figure 7(c). With further prolonging growth time, the inward-tilt (100) facets continuously expand upwards and intersect each other. The intersections result in significant changes in sizes and shapes of outward-tilt (100) facets and (111) facet. Obviously, the outward-tilt (100) facets grow up to the maximum size and present an equilateral triangle profile at the moment of the emergence of inward-tilt (100) intersection. And at the same time, the (111) facet being in shrinking takes final shape from hexagon into equilateral triangle. Then, companying with the increasing of inward tilt (100) face size in vertical direction, the triangle (111) face gradually declines with increasing growth time, and completely vanishes after 180 mins, finally forming a pyramidal structure with six (100) facets, as shown in figure 7(e). The size and shape of the

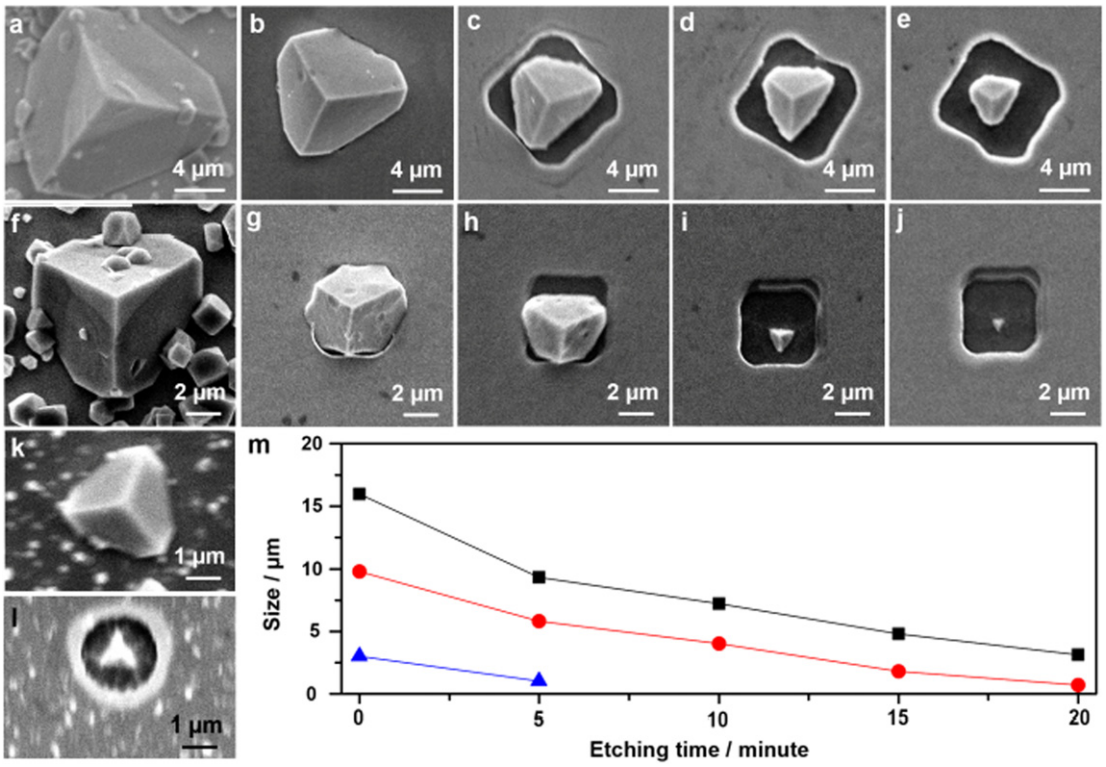

Figure 6. Etching time dependence of 3D PbSe pyramid size. A continuous size decrease was observed both from large (a)–(e), medium (f)–(j) and (k)–(l) small PbSe pyramids grown from 8 × 8 μm, 5 × 5 μm square hole and 2 μm diameter round hole masks, respectively, with increasing etching time from (b) (g) and (l) 5 mins, (c) and (h) 10 mins, (d) and (i) 15 mins, to (e) and (j) 20 mins.

outward-tilt (100) facets remain unchanged before the tip is formed. By further increasing growth time, the pyramid becomes bigger and bigger by an isotropic growth method. It should be noticed that on the surface of Au mask only sporadic small-size PbSe crystallites with random orientation were grown. This is because it is difficult to form PbSe nucleation on gold surface duo to chemical inert of bulk gold [36].

In order to discuss the growth mechanism, we propose that the multi-facet PbSe pyramid shown in figure 7(g) was formed by the Confined-Oriented-Attachment (COA) mechanism in the multi-component growth system. Current, The Oriented Attachment (OA) mechanism [37, 38] is a special oriented attachment mechanism following the Gibbs-Curie-Wulff (GCW) minimum energy principle [39]. It is well known that nonpolar {100} facets of the PbSe crystal are the most stable surfaces with a lowest surface energy of 0.184 Jm-2 [40], while the {110} and {111} facets have surface energies of 0.318 and 0.328 Jm-2, respectively. Therefore, to follow the general GCW minimum energy principle, the cubic shape of an equilibrium PbSe crystal will be synthetized by minimizing the total surface free energy associated to the crystal-medium interface. Specifically speaking, for an unitary water solution growth system with no intentional orientation control involving, {110} and {111} facets of the PbSe material which are formed in the nucleation and the initial growth stages, will be gradually eliminated during the middle and late growth stage until six squared {100} intersect to form a most thermodynamically stable cubic shape, as depicted in figure 7(f-I). This is the reason that only poly-crystalline PbSe cubic particle packing films could be obtained from regular CBD method.

However, the introduction of (111) PbSe epitaxial layer will be able to break the equilibrium of solution growth system, resulting in the formation of a non-equilibrium PbSe single-crystal film of (111) orientation with a higher surface energy. In our opinion, the survived (111) facet is attributed to the two-dimensional regular oriented attachment (2D-OA) mechanism as shown in figure 7(f-II) [41]. This OA mechanism is now widely recognized as a key process in the solution-phase growth of crystals with various nanostructures, whereby nano-crystal units with special shapes interact and aggregate along specific crystallographic direction to form hierarchical nanostructures, such as spheres, ellipsoids, platelets, wire, hybrids. In our case, the surface of (111) PbSe epitaxial layer has only one kind of element layer on top which is either Pb or Se atomic layer. This kind of atomic arrangement decides the initial nucleation and growth of PbSe crystals on the (111) epitaxial dominantly via an atomic layer-by-layer deposition. Therefore, the atomic arrangement and the (111) orientation of epitaxial layer will be copied to the fresh PbSe nano-crystals due to the layer-by-layer deposition method. Furthermore, to also follow the GCW minimum energy principle, the PbSe nano-crystals are of pyramid shape

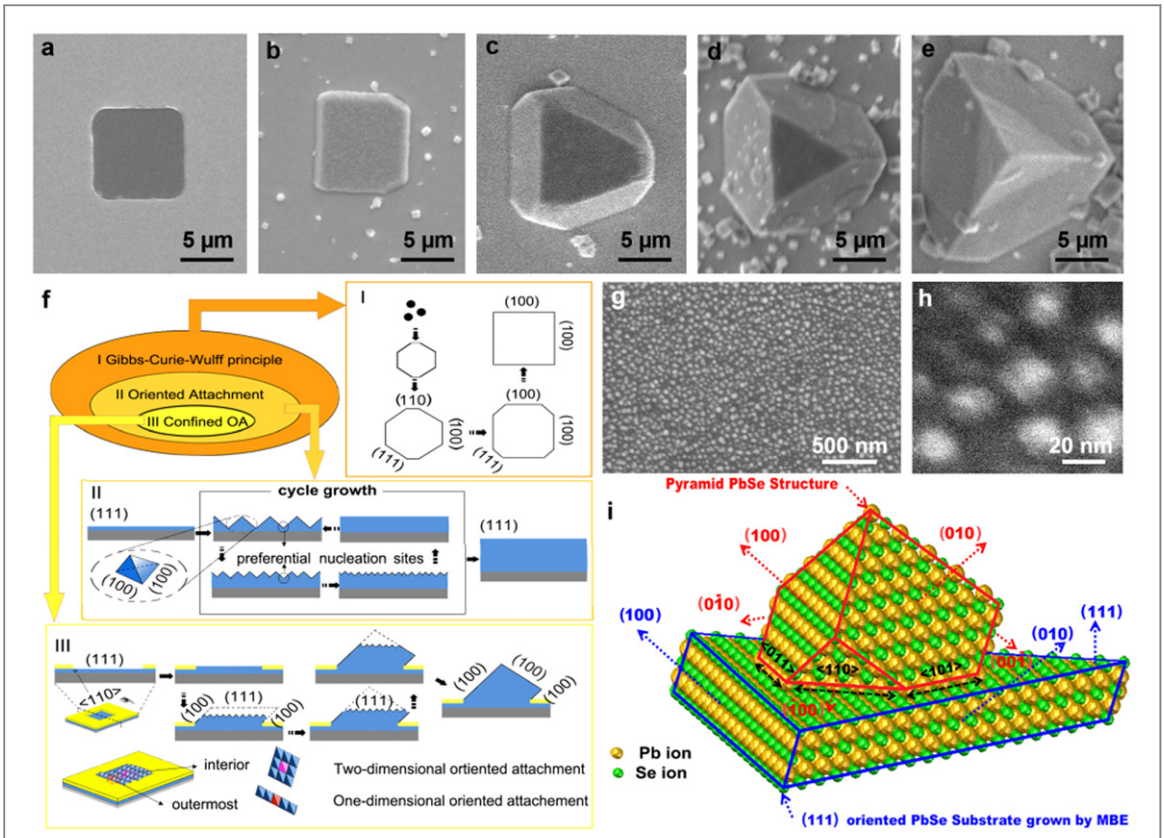

Figure 7. Morphological evolution and growth orientation of PbSe pyramid grown on Au patterned MBE-(111) buffer layer by using selective CBD epitaxial self-assemble growth. FESEM images obtained from (a) 0, (b) 15, (c) 30, (d) 90 and (e) 180 mins. (f) Schematic illustrations for the growth mechanism. (g) high- and (h) ultra-high magnification FESEM images of PbSe pyramids formed by CBD method on the (111) epitaxial layer in the initial growth stage. 3D atomic arrangement model of PbSe pyramid grown on (111) PbSe epitaxial layer.

constructed by predominantly {100} facets with the same orientation as the original epitaxial layer has, as shown in figure 7(f-II) and figures 7(g) and (h). Nevertheless, even every 20 nm-scaled PbSe pyramid constructed by three {100} triangle facets has lowest surface energy, the increase of whole surface area, is larger than the surface area of (111) epitaxial layer. It is well known that surface area and surface energy are the two factors affecting the system energy. Therefore, although {100} surface is of lowest surface energy, the increased surface energy ratio of pyramid structure still makes the whole system energy higher than that of original (111) epitaxial layer, being in unstable stage. In order to low the system energy, the PbSe nano-pyramids try to merge together with surrounding adjacent pyramids to decrease the gross area of {100} facets, as demonstrated in figure 7(f-II). The mergence is possibly realized by forming secondary PbSe pyramids between the existing PbSe pyramids, as shown in figure 7(f-II). This is due to that the valleys between pyramids provide preferential sites for nucleation and growth because of higher bonding density. This mergence process will keep on until a new flat (111) PbSe epitaxial layer emerges. Therefore, the fresh (111) epitaxial layer by chemical reaction is self-assembled by 2D-OA mechanism of hierarchical PbSe nano-pyramids along (111) direction. The self-assembly procedure described above will repeat till the reactants in precursor are consumed out, resulting in forming a thick epitaxial layer with a quick growth rate.

In order to realize COA growth mechanism, an Au masking process has to be involved. Due to the well-known chemical inactivity of Au and its lattice mismatch with PbSe, the nucleation and growth can hardly happen at gold surface. After the thickness of fresh (111) epitaxial layer exceeds the thickness of Au mask, the absence of PbSe pyramids on Au coating determines that the emerged outermost (100) facets of nano-scale pyramids close to the Au mask only adopts one-dimensional oriented attachment (1D-OA) along <110> direction, and eventually form a large (100) facet, as shown in figure 7(f-III). However, the (100) facets of interior nano-pyramids vanish by 2D-OA mechanism to form fresh (111) facet, bring a lowest energy system. Finally, large size PbSe pyramids were formed on the confined positions under the dual functions of 1D- and 2D-OA.

It is necessary to predict that a perfect pyramid shape structure of PbSe with only three inward-tilted (100) facets should be achieved if a mask with equilateral triangular opening areas is used for lithographic process and also all three triangle's sidelines can match with three [110] interconnection lines between {111} surface and the

original epitaxial layer's (111) surface. Due to the fact that these three inward-tilted (100) facets have interconnected with each other at the very beginning of the CBD growth procedure. However, in the case shown in figure 7, the mask used is of square shape. Therefore, three major inward-tilted {100} surfaces have been separated by other facets from the beginning of the CBD growth as shown in figure 7(b). Based on the GCW minimum energy principle, it is suggested that the separation facets between these three major inward-tilted {100} facets are the rest three {100} facets that is outward-tilted with their orientation facing downwards to the wafer since their surface energies are lower than other facets. And as just stated, while the growth process is proceeding, the top three{100} surfaces will keep growing to get connected as shown in figure 7(d), and the (111) higher energy surface will keep shrinking and eventually be disappeared to form a pyramid head as can be seen in figure 7(e).

4. Conclusions

In summary, we have devised a template assembly route yielding 3D highly faceted single-crystal PbSe pyramidal arrays from selective chemical bath deposition. Every PbSe pyramid is enclosed by six lowest free-energy {100} surface planes, and these facets are all aligned parallel to the sixfold (110) directions within the (111) surface plane. The size of PbSe pyramids could be well tailored by the size of pre-organized Au pattern and the etching time. PbSe pyramids were formed on the confined positions under the dual functions of 1D- and 2D-OA following the Gibbs-Curie-Wulff minimum energy principle. The arrayed nature and narrow size distribution of the assembled structures provide an excellent platform for advancing applications and assembly processes reliant on the unique properties of PbSe. It is predictable that epitaxial pyramid arrays are likely to be obtained using an elegant single step chemical epitaxy deposition (without MBE-PbSe seed layer) on GaAs or surface treatment Si substrates by COA mechanism based on the Dr Golan's studies [30–35] on the lead-salt epitaxial thin films from CBD.

Acknowledgments

We acknowledge financial supports under DoD ARO Grant No. W911NF-14-1-0312, Oklahoma OCAST program under Grant Nos. AR132-003 and AR14-035.

References

[1] Zhou W and Wang Z L 2011 *Three-Dimensional Nanoarchitectures: Designing Next-Generation Devices* (New York: Springer)
[2] Green M A 1993 Silicon solar cells: evolution, high-efficiency design and efficiency enhancement *Semicond Scl Techno1* **8** 1–12
[3] He L, Lai D, Wang H and Jiang C 2012 High-efficiency Si/polymer hybrid solar cells based on synergistic surface texturing of Si nanowires on pyramids *Small* **8** 1664–8
[4] Sun J, Choi K and Lee U 2012 Fabrication of pyramidal corrugated quantum well infrared photodetector focal plane arrays by inductively coupled plasma etching with BCl_3/Ar *J Micro/Nanolith MEMS MOEMS* **11** 043003 1- 4
[5] Ho S J, Kim J U, Song Y H, Kim B J, Ryu C J and Lee J L 2012 Design rule of nanostructures in light-emitting diodes for complete elimination of total internal reflection *Adv. Mater.* **24** 2259–62
[6] Bae S Y, Kim D H, Lee D S, Lee S J and Baek J H 2012 Highly integrated InGaN-GaNSemipolar micro-pyramid light-emitting diode arrays by confined selective area growth *Electrochem Solid-State Lett* **15** H47–50
[7] Fan F R, Lin L, Zhu G, Wu W, Zhang R and Wang Z L 2012 Transparent triboelectric nanogenerators and self-powered pressure sensors based on micropatterned plastic films *Nano Lett.* **12** 3109–14
[8] Baker-Finch S C and McIntosh K R 2011 Reflection of normally incident light from silicon solar cells with pyramidal texture *Prog photovolt* **19** 406–16
[9] Choi J J *et al* 2011 Nearly single-crystalline GaN light-emitting diodes on amorphous glass substrates *Nat. Photonics* **5** 763–9
[10] Donnellya V M and Kornblitb A 2013 Plasma etching: yesterday, today, and tomorrow *J. Vac. Sci. Technol.*A **31** 050825 1-48
[11] Li X 2012 Metal assisted chemical etching for high aspect ratio nanostructures: a review of characteristics and applications in photovoltaics curr. opin. *Solid State Mater. Sci.* **16** 71–81
[12] Jansen H, Gardeniers H, Boer M, Elwenspoek M and Fluitman J 1996 A survey on the reactive ion etching of silicon in microtechnology *J. Micromech. Microeng.* **6** 14–28
[13] Wortmann D, Gottmann J, Brandt N and Horn-Solle H 2008 Micro- and nanostructures inside sapphire by Fs-laser irradiation and selective etching *Optics Express* **16** 1517–22
[14] Ertorer E, Vasefi F, Keshwah J, Najiminaini M, Halfpap C, Langbein U, Carson J L, Hamilton D W and Mittlerb S 2013 Large area periodic, systematically changing, multishape nanostructures by laser interference lithography and cell response to these topographies *J Biomed Opt.* **18** 035002 1-8
[15] Khokhlov D 2003 *Lead Chalcogenides: Physics and Applications* (New York: Taylor& Francis)
[16] Kapon E 1999 *Semiconductor Lasers: Materials and Structures* (San Siego: Academic Press)
[17] Liang W, Rabin O, Hochbaum A I, Fardy M, Zhang M and Yang P 2009 Thermoelectric properties of p-type PbSe nanowires *Nano. Res.* **2** 394–9
[18] Rogalski A 2003 Infrared detectors: status and trends *Prog. Quantum Electron.* **27** 59–210
[19] Semonin O E, Luther J M, Choi S, Chen H Y, Gao J, Nozik A J and Beard M C 2011 Peak external photocurrent quantum efficiency exceeding 100% via MEG in a quantum dot solar cell *Science* **334** 1530–3

[20] Ellingson R J, Beard M C, Johnson J C, Yu P, Micic O I, Nozik A J, Shabaev A and Efros A L 2005 Highly efficient multiple exciton generation in colloidal PbSe and PbS quantum dots *Nano Lett.* **5** 865–71
[21] Mukherjee S, Li D, Gautam A, Kar J P and Shi Z 2010 *Lead Salt Thin Film Semiconductors for Microelectronic Applications* (Kerala: Research Signpost) ISBN: 978-81-7895-501-8
[22] Gorer S, Albu-Yaron A and Hodes G 1995 Chemical solution deposition of lead selenide films: a mechanistic and structural study *Chem. Muter.* **7** 1243–56
[23] Li C, Bai T, Li F, Wang L, Wu X, Yuan L, Shi Z and Fenga S 2013 Growth orientation, shape evolution of monodisperse PbSe nanocrystalsand their use in optoelectronic devices *CrystEngComm* **15** 597
[24] Bealing C R, Baumgardner W J, Choi J J, Hanrath T and Hennig R G 2012 Predicting nanocrystal shape through consideration of surface-ligand interactions *ACS Nano.* **6** 2118–27
[25] Choi J J *et al* 2009 PbSe nanocrystal excitonic solar cells *Nano. Lett.* **9** 3749–55
[26] Cao H, Gong Q, Qian X, Wang H, Zai J and Zhu Z 2007 Synthesis of 3-D hierarchical dendrites of lead chalcogenides in large scale via microwave-assistant method *Cryst. Growth Des.* **7** 425–9
[27] Lu W, Fang J, Wang Y and Lin Z 2005 Formation of PbSe nanocrystals: a growth toward nanocubes *J. Phys. Chem.*B **109** 19219–22
[28] Cho K S, Talapin D V, Gaschler W and Murray C B 2005 Designing PbSe Nanowires and nanorings through oriented attachment of nanoparticles *J. Am. Chem. Soc.* **127** 7140–7
[29] Ma J G, Curtis M E, Zurbuchen M A, Keay J C, Weng B B, Li D H, Zhao F H, Johnson M B and Shi Z 2010 Growth mechanism of cuboid growth pits in lead selenide epilayers grown by molecular beam epitaxy *J. Phys. D: Appl. Phys.* **43** 455411 1-6
[30] Osherov A, Shandalov M, Ezersky V and Golan Y 2007 EPITAXY and orientation control in chemical solution deposited PbS and PbSe monocrystalline films *J. Cryst. Growth* **304** 169–78
[31] Osherov A, Ezersky V and Golan Y 2012 Hetero-twinning in chemical epitaxy of PbS thin films on GaAs substrates *Cryst. Growth Des.* **12** 4006–11
[32] Shandalov M and Golan Y 2003 Microstructure and morphology evolution in chemical solution deposited pbse films on GaAs (100) *Eur. Phys. J Appl. Phys.* **24** 13–20
[33] Shandalov M and Golan Y 2005 Microstructure and morphology evolution in chemical solution deposited semiconductor films: 3 PbSe on GaAs vs Si substrate *Eur. Phys. J. Appl. Phys.* **31** 27–30
[34] Templeman T, Biton M, Safrani T, Shandalov M, Yahel E and Golan Y 2014 Chemically deposited PbSe thin films: factors deterring reproducibility in the early stages of growth *CrystEngComm* **16** 10553–9
[35] Osherov A and Golan Y 2010 Chemical epitaxy of semiconductor thin films *MRS Bull.* **35** 790–6
[36] Haruta M 2003 When gold is not noble: catalysis by nanoparticles *The Chemical Record* **3** 75–87
[37] Raju M, Duin A C T and Fichthorn K A 2014 Mechanisms of oriented attachment of TiO_2 nanocrystals in vacuum and humid environments: reactive molecular dynamics *Nano Lett.* **14** 1836–42
[38] Zhang J, Huang F and Lin Z 2010 Progress of nanocrystalline growth kinetics based on oriented attachment *Nanoscale* **2** 18–34
[39] Benz K W and Neumann W 2014 *Introduction to Crystal Growth and Characterization* (Singapore: Markono Print Meida Pte Ltd)
[40] Fang C, Huis M A, Vanmaekelbergh D and Zandbergen H W 2010 Energetics of polar and nonpolar facets of PbSe nanocrystals from theory and experiment *ACS Nano.* **4** 211–8
[41] Schliehe C *et al* 2010 Ultra-thin PbS sheets by two-dimensional oriented attachment *Science* **329** 550–3